

# Dilute moment n-type ferromagnetic semiconductor Li(Zn,Mn)As

J. Mašek,<sup>1</sup> J. Kudrnovský,<sup>1</sup> F. Máca,<sup>1</sup> B. L. Gallagher,<sup>2</sup> R. P. Campion,<sup>2</sup> D. H. Gregory,<sup>3</sup> and T. Jungwirth<sup>4,2</sup>

<sup>1</sup>*Institute of Physics ASCR, Na Slovance 2, 182 21 Praha 8, Czech Republic*

<sup>2</sup>*School of Physics and Astronomy, University of Nottingham, Nottingham NG7 2RD, UK*

<sup>3</sup>*Department of Chemistry, University of Glasgow, Glasgow G12 8QQ, UK*

<sup>4</sup>*Institute of Physics ASCR, Cukrovarnická 10, 162 53 Praha 6, Czech Republic*

We propose to replace Ga in (Ga,Mn)As with Li and Zn as a route to high Curie temperature, carrier mediated ferromagnetism in a dilute moment n-type semiconductor. Superior material characteristics, rendering Li(Zn,Mn)As a realistic candidate for such a system, include unlimited solubility of the isovalent substitutional Mn impurity and carrier concentration controlled independently of Mn doping by adjusting Li-(Zn,Mn) stoichiometry. Our predictions are anchored by detail *ab initio* calculations and comparisons with the familiar and directly related (Ga,Mn)As, by the microscopic physical picture we provide for the exchange interaction between Mn local moments and electrons in the conduction band, and by analysis of prospects for the controlled growth of Li(Zn,Mn)As materials.

PACS numbers: 75.50.Pp, 75.30.Hx, 73.61.Ey

(Ga,Mn)As is a prototypical of a unique class of spintronic materials in which ferromagnetic coupling between dilute local moments is mediated by semiconductor band carriers.<sup>1,2</sup> This unusual behavior is realized in the conventional semiconductor GaAs using only one type of dopant, Mn<sub>Ga</sub>, which provides both local spins and holes. The simplicity of such a system inevitably brings also limitations to the structural, ferromagnetic and semiconducting properties due to the low solubility of Mn and due to the lack of independent control of local moment and carrier densities. Among the negative consequences are Curie temperatures below room temperature, and p-type conduction only. In our study we predict that these limitations can be lifted by a straightforward substitution of the group-III element Ga with group-I Li and group-II Zn elements.

LiZnAs is a stable direct-gap semiconductor which can be grown by the high temperature reaction of elemental Li, Zn, and As.<sup>4,7</sup> Its crystal structure and band structure are very similar to those of GaAs. As shown in Fig. 1(a) and (b), the LiZnAs tetrahedral lattice can be viewed as a zincblende ZnAs binary compound, analogous to GaAs, filled with Li atoms at tetrahedral interstitial sites near As. The relatively small first ionization energy of Li makes the (Li)<sup>+</sup>(ZnAs)<sup>-</sup> compound half ionic and half covalent.<sup>3</sup> The measured band gap of LiZnAs (1.61 eV) is very similar to the GaAs band-gap (1.52 eV).<sup>5</sup> An overall similarity of the LiZnAs and GaAs electronic structures, including valence band and conduction band dispersions, ground state charge density, and phonon dispersion relations has been reported in *ab initio* local-density-approximation (LDA) studies.<sup>3,6</sup>

Application of the LDA description of the electronic band-structure to Mn-doped zincblende semiconductors runs into a conceptual difficulty in dealing with local moment levels coincident with itinerant electron bands. To partly remedy this inadequacy of standard first principles approaches we use in this paper the LDA+U technique which combines LDA with the Hubbard descrip-

tion of strongly correlated localized orbitals.<sup>8,9,10,11</sup> The LDA+U method is implemented within the framework of the first-principles, tight-binding linear muffin-tin orbital approach; disorder effects associated with random distribution of Mn and other defects if present are accounted for using the coherent potential approximation (CPA).<sup>12</sup>

In Fig. 1(c) and (d) we compare LDA+U/CPA density of states (DOS) of LiZnAs and GaAs doped with 5% of Mn. Since Mn introduces one hole per Mn in GaAs but is isovalent in LiZnAs, the structure considered in Fig. 1(d) is Li<sub>0.95</sub>(Zn<sub>0.95</sub>Mn<sub>0.05</sub>)As to allow for a direct comparison of p-type ferromagnets realized in the two hosts. As expected from the similar host band structures and nearly atomic-like character of Mn *d*-states in (moderately) narrow-gap zincblende semiconductors,<sup>13</sup> both systems are ferromagnetic with comparable valence-band exchange splittings and similar Mn *d* and host *sp*-projected DOSs. In particular, the main peak in the majority-spin *d*-orbital DOS is well below the valence band edge resulting in states near the Fermi energy having a predominantly As *p*-character in both systems.

The LDA+U/CPA band structure of (Ga,Mn)As is consistent with a number of experiments in this ferromagnetic semiconductor.<sup>2</sup> We expect, based on the above similarities between the two systems, that Li(Zn,Mn)As is also described reliably by this theoretical technique. In the following paragraphs we use the *ab initio* band structures to explore Li(Zn,Mn)As mixed crystals over a wide range of local moment and carrier dopings, including regimes which are technologically inaccessible in the GaAs host. In particular, we focus on the equilibrium solubility of isovalent Mn in LiZnAs for concentrations well above 1% and on ferromagnetism in LiZnAs with n-type conduction which, as we show, can be readily achieved without introducing any additional chemical elements.

The calculated formation energies of Mn<sub>Zn</sub> are plotted in Fig. 2(a) for insulating stoichiometric Li(Zn,Mn)As, for p-type Li(Zn,Mn)As with Li vacancies, and for n-type Li(Zn,Mn)As with additional Li<sub>I</sub> atoms occupying

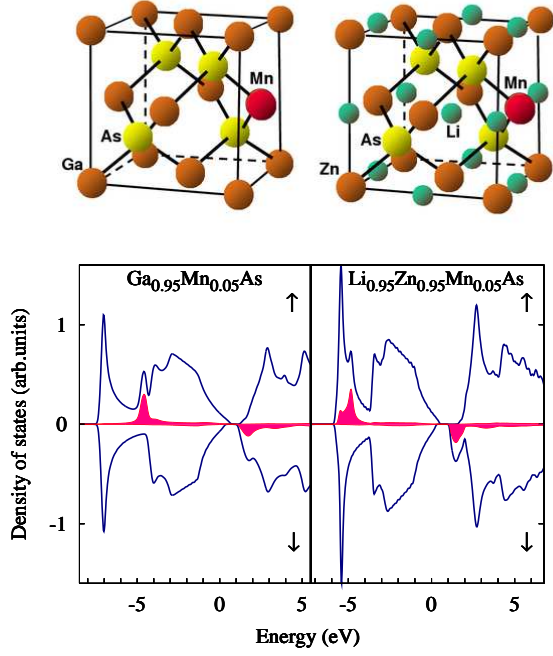


FIG. 1: Top panel: Schematics of (Ga,Mn)As and Li(Zn,Mn)As crystal structures. Bottom panel: *ab initio* total (blue lines) and Mn *d*-orbital projected (red filled lines) density of states of Ga<sub>0.95</sub>Mn<sub>0.05</sub>As and Li<sub>0.95</sub>(Zn<sub>0.95</sub>Mn<sub>0.05</sub>)As mixed crystals. Energy on the *x*-axis is measured from the Fermi energy.

tetrahedral interstitial sites near Zn. Independent of the charge doping, the formation energy of Mn<sub>Zn</sub> is negative, i.e., we find no equilibrium solubility limit for substitutional Mn<sub>Zn</sub>, consistent with its isovalent nature. (Note that we focus in this paper on dilute Mn systems far from the LiMnAs limit; the LiMnAs compound is an antiferromagnet<sup>14,15</sup> due to short-range Mn-Mn superexchange.) This result contrasts with the positive formation energy of Mn<sub>Ga</sub> in GaAs<sup>16</sup> which leads to an equilibrium solubility limit below 1%.

A detailed analysis of non-stoichiometric n-type Li(Zn,Mn)As is presented in Figs. 2(b)-(d). Panel (b) demonstrates that in systems with over-stoichiometric Li concentrations a large number of Li<sub>I</sub> atoms can be incorporated at interstitial sites near Zn. Formation energy of these single-donor impurities is negative and decreases with increasing Mn doping.

In covalent semiconductors, carrier doping is limited due to strong tendency to self-compensation. In the LiZnAs host with excess Li, Li<sub>Zn</sub> antisites represent natural single-acceptor defects compensating the interstitial Li<sub>I</sub> donors. *Ab initio* calculations of formation energies can be used<sup>16,17</sup> to estimate the dependence of Li<sub>I</sub> and Li<sub>Zn</sub> partial concentrations on the total density of excess Li atoms above the Li-(Zn,Mn) stoichiometry. Results are plotted in Figs. 2(c) and (d) for Mn doping of 5% and 12.5%, respectively. Although the tendency to self-compensation is clearly apparent, the theoretical data

suggest that large net electron densities are feasible in Li(Zn,Mn)As owing to the partly ionic character of the compound. Remarkably, the n-type doping efficiency by excess Li increases significantly with increasing Mn concentration.

We now consider the magnetic properties of Li(Zn,Mn)As semiconductors. The compatibility of the CPA with Weiss mean-field theory allows us to estimate the strength of Mn-Mn magnetic coupling, at a given chemical composition, from the calculated energy cost,  $E_{rev}$ , of reversing one Mn moment with all other Mn moments aligned.<sup>18,19</sup> Results for  $E_{rev}$  shown in Fig. 3(a) were obtained using a rigid-band approximation. Here the LDA+U/CPA band structure was calculated in one charge state of the compound only, and the dependence on carrier doping was obtained by shifting the Fermi energy while keeping the bands fixed. Note that for the 5% Mn doping considered in the figure, carrier doping of -5% corresponds to one hole per Mn and +5% to one electron per Mn. Open and closed squares represent  $E_{rev}$  obtained applying the above rigid band scheme, based on n-type Li<sub>1.05</sub>(Zn<sub>0.95</sub>Mn<sub>0.05</sub>)As and p-type Li<sub>0.95</sub>(Zn<sub>0.95</sub>Mn<sub>0.05</sub>)As band structures, respectively. The similarity of the two curves indicates that the position of the Fermi energy plays the dominant role in magnetic interactions while disorder effects associated with non-stoichiometric Li-(Zn,Mn) configurations are less important. For comparison we plot in Fig. 3(a) the rigid band  $E_{rev}$  obtained from the Ga<sub>0.95</sub>Mn<sub>0.05</sub>As *ab initio* band structure (see also Ref. 20). As expected the two compounds show very similar magnetic behavior.

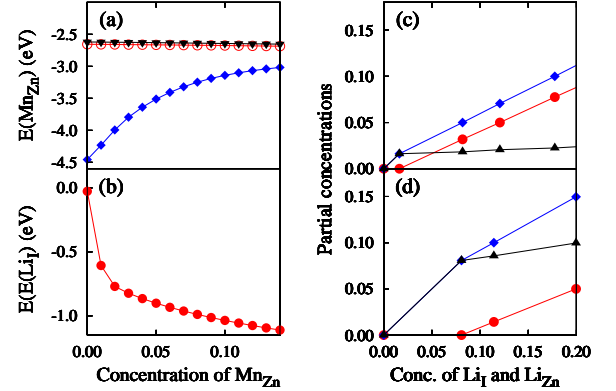


FIG. 2: *Ab initio* impurity formation energies of Li(Zn,Mn)As mixed crystals: (a) Mn<sub>Zn</sub> formation energy as a function of Mn<sub>Zn</sub> doping for stoichiometric structures (red open dots), for p-type systems with 5% of Li vacancy acceptors (black triangles), and for n-type systems with 5% of donor Li<sub>I</sub> impurities occupying Zn-tetrahedral interstitial sites (blue diamonds). (b) Li<sub>I</sub> formation energy near the stoichiometric composition as a function of Mn<sub>Zn</sub> doping. (c) Partial concentration of Li<sub>I</sub> (blue diamonds) donors, Li<sub>Zn</sub> acceptors (red dots), and net electron doping (black triangles) for 5% of Mn<sub>Zn</sub> as a function of total concentration of excess Li (Li<sub>I</sub> plus Li<sub>Zn</sub>). (d) Same as (c) for 12.5% of Mn<sub>Zn</sub>.

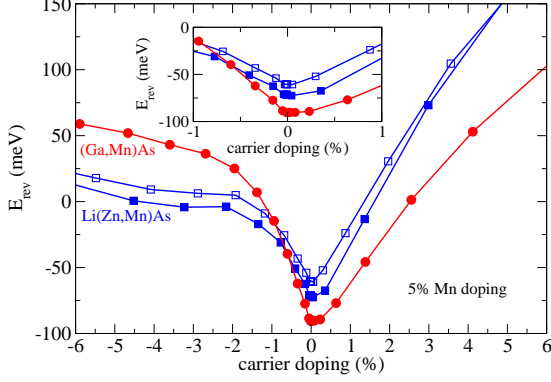


FIG. 3: Energy cost of flipping one Mn moment calculated with all other Mn moments aligned. Open and closed squares were obtained from n-type  $\text{Li}_{1.05}(\text{Zn}_{0.95}, \text{Mn}_{0.05})\text{As}$  and p-type  $\text{Li}_{0.95}(\text{Zn}_{0.95}, \text{Mn}_{0.05})\text{As}$  *ab initio* band structures, respectively (see text for details). Circles represent calculations for  $\text{Ga}_{0.95}\text{Mn}_{0.05}\text{As}$ .

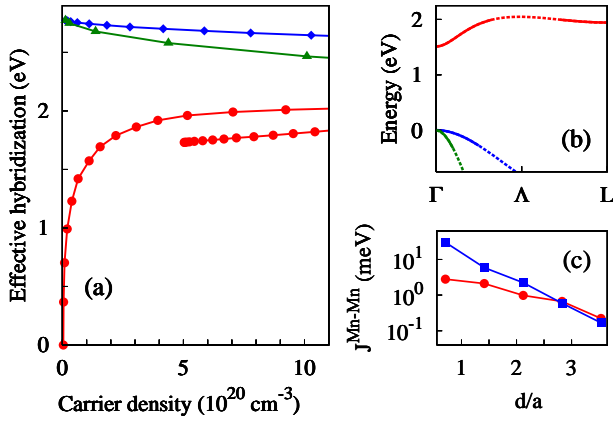


FIG. 4: (a) Model calculations of  $\text{Mn}_{\text{Ga}}$   $d$ -orbital hybridization potentials with GaAs  $sp$ -orbitals at the Fermi energy in the valence band (blue diamonds and green triangles) and conduction band (red dots) as a function of hole density and electron density, respectively. (b) Model band structure of the GaAs host illustrating the filled conduction band states (red full line) and empty valence band states (black and blue lines) for electron or hole density of  $10^{21} \text{ cm}^{-3}$  (largest carrier density considered in panel (a)). (c) *Ab initio* Mn-Mn exchange interactions as a function of Mn interatomic distance evaluated along the  $[110]$  crystal direction.

The calculated positive values of  $E_{\text{rev}}$  at large hole concentrations correspond to ferromagnetic Mn-Mn coupling, which is consistent with experimentally observed ferromagnetic ground states in highly doped p-type (Ga,Mn)As. (At low enough hole concentrations,  $E_{\text{rev}}$  changes sign and ferromagnetism becomes unstable due to the dominant role of short-range antiferromagnetic Mn-Mn superexchange.<sup>2</sup>) The comparable strength of ferromagnetic Mn-Mn coupling for n-type and p-type doping at high carrier concentrations suggests that exchange interactions between Mn  $d$ -states and conduction band states in zincblende semiconductors can be strong

and that  $\text{Li}(\text{Zn}, \text{Mn})\text{As}$  with properly adjusted stoichiometry is a high Curie temperature n-type ferromagnetic semiconductor.

We now discuss the physical origin of the high temperature electron-mediated ferromagnetism. In zincblende semiconductors doped with Mn  $d^5$  impurities, the local moments can have either a direct exchange interaction with band electrons on the same site and/or an interaction due to  $sp-d$  hybridization between the Mn local moment and band electrons on neighboring sites.<sup>21,22</sup> The latter interaction is much stronger and high-temperature ferromagnetism is expected to occur only when the hybridization coupling mechanism is present. In GaAs, the valence band edge at the  $\Gamma$ -point has a  $p$ -orbital character with a larger contribution from As.<sup>23</sup> Since the density of states at the valence band edge is large, the occupied states for typical hole densities in ferromagnetic (Ga,Mn)As are still close to the  $\Gamma$ -point and have similar atomic orbital composition. The  $p-d$  hybridization is allowed by symmetry within the whole Fermi sea (including the  $\Gamma$ -point) which, together with the large magnetic susceptibility of heavy mass holes, explains the experimentally observed robust ferromagnetism in p-type (Ga,Mn)As.

The bottom of the conduction band of GaAs has an  $s$ -orbital character with a larger contribution from Ga. The smaller admixture of orbitals from the nearest neighbor As atoms to  $\text{Mn}_{\text{Ga}}$ , the vanishing  $s-d$  hybridization at the  $\Gamma$ -point due to symmetry, and the small magnetic susceptibility of low effective mass electrons near the bottom of the conduction band all suggest that ferromagnetism is unfavorable in n-type systems. As shown in the inset of Fig. 3, a weaker tendency towards ferromagnetism in n-type materials is indeed observed in our *ab initio* calculations, however, is limited to relatively low electron dopings.

To explain the seemingly unexpected robust ferromagnetism at larger electron concentrations we present, in Fig. 4(a) and (b), tight-binding model calculations of the energy dependent  $sp-d$  hybridization potential in the conduction band and compare with the more familiar valence band case. When moving off the  $\Gamma$ -point, the hybridization rapidly sets in partly due to the  $s-d$  hybridization allowed by symmetry at non-zero wavevectors and partly due to the admixture of As and Ga  $p$ -orbitals which increases with increasing wavevector. The strength of the  $sp-d$  hybridization in highly doped n-type systems becomes comparable to that of p-type materials as the Fermi energy leaves the bottom part of the conduction band and approaches the  $L$ -point. The same picture, which we have discussed for the more familiar GaAs host doped with Mn, applies to  $\text{Li}(\text{Zn}, \text{Mn})\text{As}$  whose material properties, as analyzed above, are much more favorable for achieving large n-type doping.

Within the mean-field theory, the ferromagnetic Curie temperature,  $T_c$ , can be estimated as  $T_c \approx E_{\text{rev}}/6k_B$ , where  $k_B$  is the Boltzmann constant. The mean-field approximation should be reliable when the carrier medi-

ated Mn-Mn coupling is sufficiently long range but tends to overestimate  $T_c$  when the carriers become more localized and magnetic interactions short-ranged.<sup>24,25,26</sup> In Fig. 4(c) we plot the spatially dependent interatomic exchange energies obtained by mapping the LDA+U/CPA total energies on the Heisenberg Hamiltonian.<sup>12</sup> As seen in the figure, the n-type Li(Zn,Mn)As shows very similar magnetic interaction characteristics to the p-type (Ga,Mn)As with corresponding doping densities. In both systems the leading exchange interactions are ferromagnetic and the interaction range safely exceeds the average Mn-Mn moment distance. Consistent with the theory expectations, experimental high quality (Ga,Mn)As materials show mean field-like magnetization curves and Curie temperatures proportional to the density of  $Mn_{Ga}$ .<sup>17</sup> Maximum  $Mn_{Ga}$  doping achieved so far is approximately 6% and the corresponding record  $T_c$  is 173 K.<sup>17</sup> Calculations shown in Fig. 4 suggest comparable Curie temperatures for the n-type Li(Zn,Mn)As counterparts. Since we found no doping limit for  $Mn_{Zn}$  in Li(Zn,Mn)As and straightforward means of high electron doping in the material, Li(Zn,Mn)As might lead not only to the realization of a high Curie temperature diluted magnetic semiconductor with electron conduction but also might allow for larger magnetic moment density and therefore larger maximum  $T_c$  than (Ga,Mn)As.

We conclude by briefly discussing prospects for the controlled growth of Li(Zn,Mn)As materials. Bulk high structural quality LiZnAs crystallites have been formed

by reaction of near equimolar elemental Li, Zn, and As.<sup>4,7</sup> The crystallites are stable in inert atmospheres but slowly oxidize in air. It is probable that Li(Zn,Mn)As crystallites could be formed in the same way. However, to obtain the required control of stoichiometry to produce the ferromagnetic semiconductors predicted by our calculations, molecular beam epitaxy (MBE) is likely required. LiZnAs has not previously been grown by MBE, presumably because non-magnetic LiZnAs does not seem to have any advantage over GaAs. The similarity of Li(Zn,Mn)As to (Ga,Mn)As suggests that it should be possible to grow Li(Zn,Mn)As by MBE; here Li can be supplied from a metal-organic gas source. Li(Zn,Mn)As could be grown by MBE on lattice matched, relaxed, (In,Ga)As epilayers on normal GaAs substrates, carrier doping achieved by careful control of the Li flux, and, furthermore, it should be possible to avoid post growth oxidation by overgrowth of the Li(Zn,Mn)As epilayers.

We acknowledge discussions with C.T. Foxon, A.H. MacDonald, J. Sinova, and support from the Grant Agency of the Czech Republic under Grant 202/05/0575 and 202/04/0583, the Academy of Sciences of the Czech Republic under Institutional Support AVOZ10100521 and AVOZ10100520, the Ministry of Education of the Czech Republic Center for Fundamental Research LC510 and COST P19 OC-150, the EPSRC under Grant GR/S81407/01, and the National Science Foundation under Grant No. PHY99-07949.

- 
- <sup>1</sup> T. Dietl, H. Ohno, F. Matsukura, J. Cibert, and D. Fer-  
rand, *Science* **287**, 1019 (2000).
  - <sup>2</sup> T. Jungwirth, J. Sinova, J. Mašek, J. Kučera, and A. H.  
MacDonald, *Rev. Mod. Phys.* **78**, 809 (2006).
  - <sup>3</sup> S.-H. Wei and A. Zunger, *Phys. Rev. Lett.* **56**, 528 (1986).
  - <sup>4</sup> R. Bacewicz and T. F. Ciszek, *Appl. Phys. Lett.* **52**, 1150  
(1988).
  - <sup>5</sup> K. Kuriyama, T. Kato, and K. Kawada, *Phys. Rev. B* **49**,  
11452 (1994).
  - <sup>6</sup> D. M. Wood and W. H. Strohmayr, *Phys. Rev. B* **71**,  
193201 (2005).
  - <sup>7</sup> K. Kuriyama and F. Nakamura, *Phys. Rev. B* **36**, 4439  
(1987).
  - <sup>8</sup> V. I. Anisimov, J. Zaanen, and O. K. Andersen, *Phys. Rev.*  
**B 44**, 943 (1991).
  - <sup>9</sup> J. H. Park, S. K. Kwon, and B. I. Min, *Physica B*  
**281/282**, 703 (2000).
  - <sup>10</sup> A. B. Shick, J. Kudrnovský, and V. Drchal, *Phys. Rev. B*  
**69**, 125207 (2004).
  - <sup>11</sup> M. Wierzbowska, D. Sanchez-Portal, and S. Sanvito, *Phys.*  
*Rev. B* **70**, 235209 (2004).
  - <sup>12</sup> J. Kudrnovský, I. Turek, V. Drchal, F. Máca, P. Wein-  
berger, and P. Bruno, *Phys. Rev. B* **69**, 115208 (2004).
  - <sup>13</sup> T. Schulthess, W. M. Temmerman, Z. Szotek, W. H. But-  
ler, and G. M. Stocks, *Nature Materials* **4**, 838 (2005).
  - <sup>14</sup> G. Achenbach and H. U. Schuster, *Z. anorg. allg. Chem.*  
**475**, 9 (1981).
  - <sup>15</sup> W. Bronger, P. Müller, R. Höppner, and H. U. Schuster,  
*Z. anorg. allg. Chem.* **539**, 175 (1986).
  - <sup>16</sup> J. Mašek, I. Turek, J. Kudrnovský, F. Máca, and  
V. Drchal, *Acta Phys. Pol. A* **105**, 637 (2004), cond-  
mat/0406314.
  - <sup>17</sup> T. Jungwirth, K. Y. Wang, J. Mašek, K. W. Edmonds,  
J. König, J. Sinova, M. Polini, N. A. Goncharuk, A. H.  
MacDonald, M. Sawicki, et al., *Phys. Rev. B* **72**, 165204  
(2005).
  - <sup>18</sup> A. I. Liechtenstein, M. I. Katsnelson, V. P. Antropov, and  
V. A. Gubanov, *J. Magn. Magn. Mater.* **67**, 65 (1987).
  - <sup>19</sup> J. Mašek, *Solid State Commun.* **78**, 351 (1991).
  - <sup>20</sup> L. M. Sandratskii and P. Bruno, *Phys. Rev. B* **66**, 134435  
(2002).
  - <sup>21</sup> A. K. Bhattacharjee, G. Fishman, and B. Coqblin, *Physica*  
**B+C 117-118**, 449 (1983).
  - <sup>22</sup> T. Dietl, in *Handbook of Semiconductors*, edited by S. Ma-  
hajan (North Holland, Amsterdam, 1994), vol. 3B, p. 1251.
  - <sup>23</sup> W. Harrison, *Electronic Structure and the Properties of*  
*Solid* (Freeman, San Francisco, 1980).
  - <sup>24</sup> K. Sato, W. Schweika, P. H. Dederichs, and H. Katayama-  
Yoshida, *Phys. Rev. B* **70**, 201202(R) (2004).
  - <sup>25</sup> L. Bergqvist, O. Eriksson, J. Kudrnovský, V. Drchal,  
P. Korzhavyi, and I. Turek, *Phys. Rev. Lett.* **93**, 137202  
(2004).
  - <sup>26</sup> G. Bouzerar, T. Ziman, and J. Kudrnovský, *Europhys.*  
*Lett.* **69**, 812 (2005).